A Novel Tool for Probing Membrane Protein Structure: Solid-State NMR with Proton Spin Diffusion and X-Nucleus Detection

Kristin K. Kumashiro,[†,‡,||] Klaus Schmidt-Rohr,[*,‡] Owen J. Murphy III,[§] Kerry L. Ouellette,[†] William A. Cramer,[⊥] and Lynmarie K. Thompson[†,§]

Contribution from the Department of Chemistry, Department of Polymer Science and Engineering, and Program in Molecular and Cellular Biology, University of Massachusetts, Amherst, Massachusetts 01003, and Department of Biological Sciences, Purdue University, West Lafayette, Indiana 47907

Received August 4, 1997

Abstract: We present a new solid-state NMR approach, based on ^{1}H spin diffusion with X-nucleus (^{15}N, ^{13}C, ^{31}P) detection, for investigating the structure of membrane proteins. For any segment with a resolvable signal in the X-nucleus spectrum, the depth of insertion into the lipid bilayer can be determined. The technique represents the adaptation of the Goldman−Shen ^{1}H spin-diffusion experiment with X-nucleus detection to proteins in hydrated lipid bilayers (>25% water by weight) in the gel state at 240 K. The experiments are demonstrated on the 21-kDa channel-forming domain of the toxin-like colicin E1 molecule incorporated into lipid vesicles. More than 32% of the protons in our sample are in mobile H_2O molecules, which can be selected efficiently by the ^{1}H T_2 filter in the Goldman−Shen sequence. The transfer of ^{1}H magnetization from mobile H_2O to the colicin E1 channel domain is 80% complete within only 5 ms. This transfer to the protein, probed by the amide ^{15}N signals, is faster than the transfer to the rigid protons on average, proving that most of the protein is preferentially located between the water and the lipid bilayer. From the spin-diffusion and dipolar-dephasing data, 60% of the 24 lysine side groups are shown to be highly mobile. Quantitative depth profiling is demonstrated using the ^{31}P in the lipid phosphate head groups and the ^{13}C nuclei in the lipid acyl chains as distance markers for the spin diffusion.

Introduction

The structure of membrane proteins in their lipid environment is difficult to characterize using X-ray diffraction or solution NMR techniques, due to problems with crystallization or solubility, respectively. The depths of membrane insertion of specific residues are important structural parameters that can be estimated, for instance, by fluorescence-quenching[1] and EPR techniques.[2] However, these experiments generally require manipulation of the protein or the membrane to attach probes to specific sites. Moreover, these non-native fluorescent groups or stable radicals are often bulky, which may limit the precision of the depth measurement and may also perturb the native structure.

Solid-state NMR can be used to characterize molecular structure in disordered and anisotropic environments, including membrane proteins inserted into hydrated lipid bilayers. With appropriate selective isotopic labeling schemes, local structure in membrane proteins can be determined with a number of strategies which measure selected distances[3−6] or torsion angles.[7,8] Complementary approaches suitable for measurements of overall structure include the measurement of helix orientations in oriented lipid membranes.[9−12]

We present a new NMR approach for characterizing membrane-protein structure by measuring the depth of residues within the membrane: The distance between the water−membrane interface and any spectrally resolved, isotopically labeled site in the protein is measured by ^{1}H spin diffusion with X-nucleus detection, as indicated schematically in Figure 1. The experiment is an adaptation of the Goldman−Shen experiment[13] with X-nucleus detection, previously used in heterogeneous polymers for domain-size measurements,[14] for protein bound to hydrated lipid vesicles. As outlined in the pulse sequence of Figure 2a, the ^{1}H "T_2 filter" (τ_d) is used to select mobile water ^{1}H

† Department of Chemistry, University of Massachusetts.
‡ Department of Polymer Science and Engineering, University of Massachusetts.
§ Program in Molecular and Cellular Biology, University of Massachusetts.
⊥ Department of Biological Sciences, Purdue University.
* To whom correspondence should be addressed.
|| Current address: University of Hawaii at Manoa, Department of Chemistry, Honolulu, HI 96822.

(1) Chattopadhyay, A.; London, E. *Biochemistry* **1987**, *26*, 39−45.
(2) Altenbach, C.; Greenhalgh, D. A.; Khorana, H. G.; Hubbell, W. L. *Proc. Natl. Acad. Sci. U.S.A.* **1994**, *91*, 1667−1671.
(3) Raleigh, D. P.; Levitt, M. H.; Griffin, R. G. *Chem. Phys. Lett.* **1988**, *146*, 71−76.
(4) Smith, S. O.; Bormann, B. J. *Proc. Natl. Acad. Sci. U.S.A.* **1995**, *92*, 488−491.
(5) Gullion, T.; Schaefer, J. *J. Magn. Reson.* **1989**, *81*, 196−200.
(6) Wang, J.; Balazs, Y. S.; Thompson, L. K. *Biochemistry* **1997**, *36*, 1699−1703.
(7) Feng, X.; Lee, Y. K.; Sandstrom, D.; Eden, M.; Sebald, A.; Levitt, M. H. *Chem. Phys. Lett.* **1996**, *257*, 314−320.
(8) Hong, M.; Gross, J. D.; Griffin, R. G.*J. Phys. Chem. B* **1997**, *101*, 5869−5874. Hong, M.; Gross, J. D.; Rienstra, C. M.; Griffin, R. G.; Kumashiro, K. K.; Schmidt-Rohr, K. *J. Magn. Reson.* **1997**, *129*, 85−92.
(9) Cross, T. A.; Opella, S. J. *Curr. Opin. Struct. Biol.* **1994**, *4*, 574−581.
(10) Bechinger, B.; Gierasch, L. M.; Montal, M.; Zasloff, M.; Opella, S. J. *Solid State Nucl. Magn. Reson.* **1996**, *7*, 185−191.
(11) Sanders, C. R.; Landis, G. C. *Biochemistry* **1995**, *34*, 4030−4040.
(12) Sanders, C. R.; Hare, B. J.; Howard, K. P.; Prestegard, J. H. *Prog. NMR Spectrosc.* **1994**, *26*, 421−444.
(13) Goldman, M.; Shen, L. *Phys. Rev.* **1966**, *144*, 321.
(14) Assink, R. A. *Macromolecules* **1978**, *11*, 1233. Egger, N.; Schmidt-Rohr, K.; Blumich, B.; Domke, W.-D.; Stapp, B. *J. Appl. Polym. Sci.* **1992**, *44*, 289−295. Wang, Y.; Chen, Q.; Zhang, X. In *Interfaces in Polymer, Ceramic, and Metal Matrix Composites*; Ishida, H., Ed.; Elsevier: Amsterdam, 1988; pp 249−257.

S0002-7863(97)02655-3 CCC: $15.00
Published on Web 05/06/1998

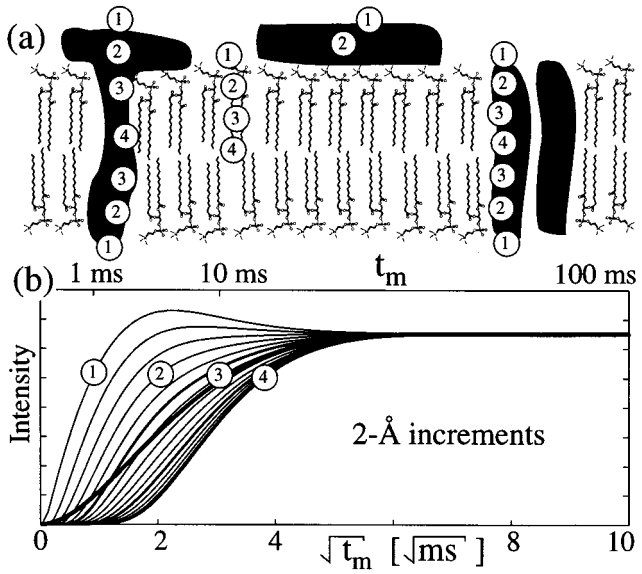

Figure 1. (a) Schematic of a section of a lipid bilayer, with surface-bound and integral protein. (b) Simulated ^{1}H spin diffusion from water at the bilayer/protein surface: time dependence of magnetization at different depths from the interface to water, with 0.2-nm increments between the curves. The parameters in the simulation were the same as in the fits to the experimental data shown in Figure 5. Numbers 1−4 in parts a and b correspond to depths of 0, 0.6, 1.5, and >2.2 nm from the water−membrane interface. The thickest line is the spin-diffusion curve for the membrane overall, which is the (rescaled) sum of all the other curves.

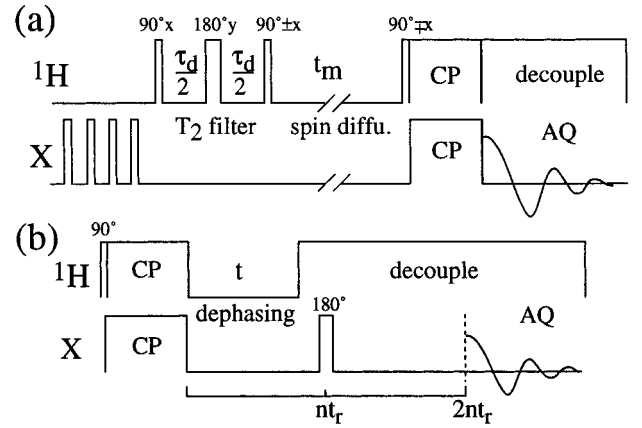

Figure 2. NMR pulse sequences used in this work. (a) Goldman−Shen spin-diffusion experiment with X-nucleus detection: initial saturation (destruction) of any ^{13}C magnetization by several 90° pulses and subsequent dipolar dephasing; selection of ^{1}H magnetization with long T_2 during the period τ_d, with a 180° pulse at $\tau_d/2$ to refocus chemical shift and field inhomogeneity; spin diffusion of ^{1}H z-magnetization during the mixing time t_m; cross-polarization from ^{1}H to the X-nucleus; and X-nucleus detection. (b) Gated-decoupling sequence, used to determine the fraction of mobile lysine side groups. Both experiments are performed with magic-angle sample spinning.

magnetization, which then spin-diffuses to the rigid protons of the protein and gel-phase lipids during the period t_m. For detection, the magnetization is transferred via cross-polarization to various X nuclei, such as ^{15}N, ^{13}C, or ^{31}P. Surprising NMR properties of the water protons under magic-angle spinning at 240 K, where the measurements were performed, are crucial in this new approach: The water is mobile enough to have a T_2 of 300 μs, yet sufficiently immobilized for efficient magnetization transfer.

The versatility of this method for observing the different components of a protein−lipid system is demonstrated here. The ^{15}N-observe experiments show that the transfer of ^{1}H magnetization to the uniformly-^{15}N-labeled 21-kDa protein is 80% complete within only 5 ms. ^{31}P in the phosphate head groups and ^{13}C sites in the acyl chains of the lipid bilayers serve as references or distance markers, which have markedly different spin-diffusion behavior; comparison of the lipid and protein spin diffusion indicates that the protein is largely surface-associated. Furthermore, the lipid data are used to calibrate detailed spin-diffusion simulations for the quantitative determination of depths of insertion of resolved sites in the protein.

The experiments are relatively straightforward to perform, using the simple pulse sequences shown in Figure 2. They can be conducted on widely available double-resonance solid-state NMR equipment, rather than the more complex and less sensitive triple-resonance equipment required for REDOR[5] and related experiments. Unlike experiments on macroscopically oriented samples, the new approach requires no special sample preparation or apparatus, except for cooling to moderately low temperatures (~240 K). Finally, different isotopic labeling schemes, such as site-specific or uniform enrichment, can be used to direct the spin-diffusion experiment to measure local or global structure, respectively.

In conjunction with the spin-diffusion work, dipolar-dephasing experiments[15] are used as an independent measurement of the mobility of various groups. ^{15}N resonances of immobile groups quickly lose intensity to dephasing by strong ^{1}H dipolar couplings, during short intervals without ^{1}H decoupling. Conversely, slow dephasing indicates weak dipolar couplings which can be due to rapid mobility. This approach has demonstrated that ca. 60% of the lysine side chains in the colicin E1 channel domain are highly mobile, presumably at the surface of the protein.

The spin-diffusion and dipolar-dephasing experiments have been applied to the channel-forming domain of colicin E1, a toxin-like protein that can exist in a soluble state and can spontaneously bind and insert into anionic membranes to form the closed state of a voltage-gated ion channel.[16] The channel domain we have studied is a 190-residue C-terminal fragment of colicin E1 (residues 333−522), also known as P190. The soluble state of this domain has been shown by X-ray crystallography[17] to consist of 10 α-helices, two of which are hydrophobic and form the core of the structure (helices 8 and 9). The membrane-bound channel-forming domain is nearly 90% α-helical, as determined by circular dichroism and infrared spectroscopy.[18] Two structural models have been proposed for the membrane-bound state, which differ with respect to membrane insertion of the hydrophobic hairpin helices. In the "umbrella" model, the hydrophobic helices traverse the bilayer with the other eight, amphipathic helices splayed on the surface, like the ribs of an open umbrella.[19] In contrast, the "penknife" model proposes that all of the helices are surface-associated.[20]

We have used spin-diffusion measurements on the uniformly-^{15}N-labeled colicin E1 channel-forming domain (P190) to

(15) Opella, S. J.; Frey, M. H. *J. Am. Chem. Soc.* **1979**, *101*, 5854−5856.
(16) Cramer, W. A.; Heymann, J. B.; Schendel, S. L.; Deriy, B. N.; Cohen, F. S.; Elkins, P. A.; Stauffacher, C. V. *Annu. Rev. Biophys. Biomol. Struct.* **1995**, *24*, 611−641.
(17) Elkins, P.; Bunker, A.; Cramer, W. A.; Stauffacher, C. V. *Structure* **1997**, *5*, 443−458.
(18) Venyaminov, S. Y.; Zakharov, S. D.; Lindeberg, M.; Griko, Y.; Salamon, Z.; Tollin, G.; Prendergast, F. G.; Cramer, W. A. *Proc. Natl. Acad. Sci. U.S.A.* **1998**, *95*, in press.
(19) Parker, M. W.; Pattus, F.; Tucker, A. D.; Tsernoglou, D. *Nature* **1989**, *337*, 93−96.

demonstrate the utility of the method for probing the structure of the membrane-bound state. These experiments determine the fraction of amide backbone nitrogens near the mobile water proton reservoir, as well as the fraction that are less accessible, such as those buried in the bilayer. Signals of nitrogen-containing side chains, such as the 24 lysines (Lys), the aromatic resonance with contributions from the three tryptophans (Trp) and two histidines (His), the side chain amide peak due to four glutamines (Gln) and 10 asparagines (Asn), and weak signals of a single arginine residue (Arg) are also observable in the ^{15}N spectrum and are used to estimate the distribution of insertion depths for these side chains.

Experimental Section

NMR. The experiments were performed on a Bruker ASX NMR spectrometer with a proton resonance frequency of 300 MHz. Bruker double-resonance magic-angle-spinning (MAS) probes (one being a triple-resonance probe used in double-resonance mode) were used with 7-mm zirconia rotors. Typical sample spinning speeds were approximately 4 kHz. Typical B_1 field strengths used in the cross-polarization were $\gamma B_1/2\pi = 40-45$ kHz, with a contact time of 1 ms. Proton decoupling during acquisition was $\gamma B_1/2\pi = 50-60$ kHz. ^{1}H 90° pulse widths used in the Goldman−Shen portion of the experiment were 6 μs. The T_2 filter, τ_d, was 200 μs for most of the measurements. Some supplementary ^{15}N data were acquired with a weaker T_2 filter of 70 μs. Typical spin-diffusion times, t_m, ranged from 0.01 to 100 ms. The cross-polarization time in all heteronuclear experiments was 1 ms. Half of this duration contributes to the actual spin-diffusion time ($=t_m + 0.5$ ms).

The dipolar dephasing experiments conducted using the pulse sequence of Figure 2b with both 1- and 3-ms contact times yielded similar decay curves for all resonances except the Lys side chains. At long dephasing times, the Lys signal retains 40% of the full CP signal at 1-ms contact time, but a larger fraction (60%) is retained in experiments with 3- and 5-ms contact times. This indicates that short contact times underestimate the mobile Lys due to its weak C−H dipolar coupling. Figure 6 below presents the 3-ms contact time data, except for the aromatic peak; the 1-ms aromatic peak data are presented because the signals are stronger and the decay appears equivalent to that at 3-ms contact time.

^{13}C chemical shifts were referenced to TMS (the methyl carbon of a *p*-di-*tert*-butylbenzene external standard was set to 31 ppm); ^{15}N chemical shifts were referenced to [^{15}N]glycine (external standard) at 32 ppm.

All NMR data were acquired at approximately 240 K. To achieve these temperatures, the bearing gas, dry air, is passed through a heat exchanger submersed in a cryofluid bath containing a CC-100II immersion cooler (NESLAB Instruments). Comparable temperature conditions were used for each set of experiments, as confirmed by measuring the width of the H_2O line in the ^{1}H spectrum (300 Hz at 240 K) and determining the reduction of the H_2O line intensity within 10 ms of spin diffusion (to ∼38%). Therefore, all reported spin-diffusion data have the same transfer rate from the mobile ^{1}H's to the rigid regions.

Production of ^{15}N-Labeled Colicin E1 Channel Domain (P190). A prototrophic strain, BM13711 (B. Wanner, Purdue University), harboring the plasmid pSKHY was used to produce ^{15}N-labeled P190. The first five residues of the P190 protein are METAE, whereas the corresponding residues in the colicin E1 molecule are LKKAQ.[21]

One liter of minimal media containing 7.0 g of K_2HPO_4, 3.0 g of NaH_2PO_4, 0.5 g of NaCl, 1.0 g of $^{15}NH_4Cl$ (Cambridge Isotope Laboratory), 2.0 g of glucose, 8.3 mg of $MgSO_4$, 100 mg of ampicillin, and trace metals[22] was inoculated with 10 mL of an overnight culture of BW13711 + pSKHY. The overnight cultures were grown in YT media (8 g/L Tryptone (Difco), 5 g/L Yeast Extract (Difco), and 2.5 g/L NaCl). The cells were grown at 37 °C with aeration by shaking to an OD_{650} of approximately 1.0, induced with 0.5 mg/L mitomycin C for 4 h, harvested and resuspended in 50 mM sodium acetate, pH 6.0, and then broken in a French pressure cell. The cell lysate was centrifuged at 14500*g* (20 min) and the supernatant applied to a CM-50 Sephadex (Pharmacia) column equilibrated with 50 mM sodium acetate, pH 6.0. The column was washed overnight with this acetate buffer, and the P190 was eluted from the column with the same buffer and 0.1 M NaCl. Fractions containing the P190 were pooled, concentrated, and dialyzed into H_2O using a Pro-Di-Con apparatus (Spectrum).

Vesicle Preparation. Synthetic dilauroylphosphatidylcholine (DLPC) and dilauroylphosphatidylglycerol (DLPG) were purchased from Avanti Polar Lipids (Alabaster, AL) in the powder form. Total lipid (200 mg) was dissolved in approximately 10 mL of chloroform in a glass test tube in a molar ratio of 2:3 DLPG:DLPC. A PG:PC ratio of 2:3 allows tight binding of the colicin E1 channel domain and high in vitro activity.[23] The chloroform was removed by evaporation with a gentle stream of filtered air, followed by vacuum desiccation for 3.5 h. The dry lipid coating on the test tube was then dissolved with vortexing in 20 mL of lipid resuspension buffer (0.1 M KCl, 10 mM dimethylglutaric acid, pH 5.0). The suspension was then subjected to five freeze−thaw cycles in the −20 °C freezer and sonicated for approximately 5 h in a bath sonicator, followed by another series of three freeze−thaw cycles.

Colicin E1 Channel Domain Binding and NMR Sample Preparation. The stock lipid suspension was diluted by a factor of 10 (to 1 mg of lipid/mL) with "binding buffer" (100 mM $NaNO_3$, 93 mM choline nitrate, 7 mM KNO_3, and 10 mM dimethylglutaric acid, pH 4.0). P190 was added at a 1:60 molar ratio of protein:lipid (12.2 mg of ^{15}N-labeled P190 in 20 mg of lipids) and incubated for 1 h on ice. The suspension of P190 bound to lipid vesicles was centrifuged in a Beckman ultracentrifuge (70Ti rotor) at 45 000 rpm for 1 h. The pellet was collected and packed into a 7-mm NMR rotor with two Kel-F spacers, so that the sample would be situated in the center of the rotor and sample coil.

Protein to lipid molar ratios ranging from 1:25 to 1:500 were analyzed previously in an IR study of secondary structure of colicin E1 channel domain, with most of the data obtained at 1:57.[24] Data obtained with this ratio seemed to fairly represent the secondary-structure content and net dichroism of the α-helicity.

Theory

In this section, we analyze the spin-diffusion process and describe the approach taken for the modeling and calibration of the experimental spin-diffusion data.

Simulation of Spin Diffusion in Hydrated Gel-Phase Membranes. ^{1}H spin diffusion is spatial diffusion of proton *z*-magnetization mediated by the ^{1}H−^{1}H dipolar coupling. The stronger the interaction, the faster the transfer and resulting spin diffusion. The spin-diffusion coefficient in typical organic solids has been measured as 0.8 ± 0.2 nm^2/ms.[25] In mobile systems, the spin diffusivity is reduced, but this reduction has been found to be less than proportional to the ^{1}H line width.[26]

Due to the well-established geometry of unilamellar lipid vesicles in H_2O, spin diffusion can be simulated efficiently and reliably. In the locally lamellar or sheetlike structure, spin diffusion is effectively a one-dimensional process along the sheet

(20) Massotte, D.; Yamamoto, M.; Scianimanico, S.; Sorokine, O.; Vandorsselaer, A.; Nakatani, Y.; Ourisson, G.; Pattus, F. *Biochemistry* **1993**, *32*, 13787−13794.

(21) Elkins, P.; Song, H. Y.; Cramer, W. A.; Stauffacher, C. V. *Proteins: Struct. Funct. Genet.* **1994**, *19*, 150−157.

(22) Anraku, Y. *J. Biol. Chem.* **1967**, *242*, 793−800.

(23) Zakharov, S. D.; Heymann, J. B.; Zhang, Y.-L.; Cramer, W. A. *Biophys. J.* **1996**, *70*, 2774−2783.

(24) Rath, P.; Bousché, O.; Merrill, A. R.; Cramer, W. A.; Rothschild, K. J. *Biophys. J.* **1991**, *59*, 516−522.

(25) Clauss, J.; Schmidt-Rohr, K.; Spiess, H. W. *Acta Polym.* **1993**, *44*, 1.

(26) Spiegel, S.; Schmidt-Rohr, K.; Boeffel, C.; Spiess, H. W. *Polymer* **1993**, *34*, 4566−4569.

normal. To be able to use different diffusion coefficients for the various layers in the structure, numerical solutions of the "discretized" spin-diffusion equation on a one-dimensional "grid" of protons, spaced by 0.2 nm, were calculated time step by time step.[27] The signal intensity of a given site is proportional to the magnetization level at the depth of that group. For a single peak reflecting various sites, for instance the unresolved methylenes along the acyl chains, the magnetization contributions from the various depths are added up in the simulation. For simulating systems with protein bound to the outer surface of the vesicle, the appropriate spin-diffusion geometry consists of an outer water layer, a protein layer, the lipid bilayer, and an inner water layer or reservoir. Due to the fast translational diffusion of the water molecules, the exact shape of the water layers is irrelevant.

The thickness of the lipid layer required for the simulations is known relatively well. Neutron scattering has shown a 5.7-nm long-period in gel-phase lipids with C_{16} acyl chains (dipalmitoylphosphatidylcholine, DPPC) and 6% H_2O.[28] In our system with C_{12} (lauroyl) acyl chains, the lipid bilayer thickness can be calculated by subtracting the 6% water (∼0.3 nm) and two times four CH_2 units (∼1.0 nm). Therefore, we used a bilayer thickness of 4.5 nm. Note that this gel-phase bilayer thickness matches the surface-to-surface thickness of 4.5 nm found by neutron scattering[29] for a lipid system in the liquid-crystalline Lα phase that can be considered as a valid model for the lipid bilayer in biomembranes. A spin-diffusion coefficient of 0.4 nm^2/ms was assumed for the protein and the lipid in the gel phase. It is reduced compared to that of rigid solids[25] due to the remaining mobility of the lipid chains in the gel phase, as indicated by the reduced (30-kHz) half-width of the broad component in the proton spectrum (see Figure 3b).

Although the spin-diffusion coefficients of the lipid and the protein are not necessarily identical, a single spin-diffusion coefficient is a reasonable approximation: The diffusion coefficient scales as (proton density)$^{1/3}$, so the diffusion coefficient would be different by only 25% for a factor-of-2 variation in proton density. Actually, in structurally heterogeneous systems, the effect of differences in proton density will be reduced because the magnetization will diffuse along paths of strong couplings around regions of low proton density, such as the protein backbone, which are therefore of little effect.

If a significant difference existed, the spin diffusion in the protein would be slower due to its lower proton density. In our data shown below, we find a faster spin diffusion to the protein backbone than to the acyl chains. This shows that the spin diffusion in the protein competes well with the spin diffusion in the lipid. For membrane-inserted proteins, transverse equilibration (at a given depth) through the relatively thin protein strands would be efficient and minimize gradients due to variations in the spin-diffusion coefficient. Relatively slow diffusion in the proton-poor phosphate head group region would be included into the relatively slow transfer from the water to the lipids. Again, on the basis of the experimental ^{31}P data (see below), we know that this transfer is actually quite efficient.

The proton spectra of water in our and various other hydrated biological systems demonstrate that the water does not freeze suddenly but that, instead, the molecular motion slows down continuously with temperature, as is typical for a supercooled melt. The freezing is quite certainly prevented by the confinement of the water molecules into thin (<3-nm) layers between the lipid bilayers. The dynamics of protons in ice, which can also be observed by NMR, do not produce as narrow a proton line as observed here.

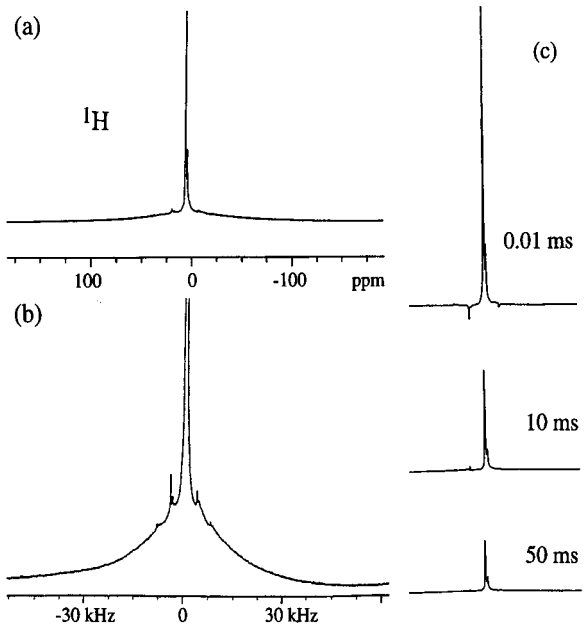

Figure 3. ^{1}H spectra of the colicin−lipid−water mixture at 240 K. (a) Spectrum to full height. (b) Close-up of the broad base of the spectrum, which arises from the immobilized protons in the lipid and protein. The narrow spikes near the top of the signal are spinning sidebands of the mobile peaks. (c) Spectra as a function of spin-diffusion time, with $\tau_d = 200\ \mu s$ T_2 selection, using the original Goldman−Shen experiment.[13]

Due to the fast diffusion of water molecules in and across the water layer, which smoothes out any magnetization gradient within microseconds, the actual thickness of the regions of mobile water does not play a role in the spin-diffusion process. What is important is the number of protons in this layer relative to the number of protons in the rigid membrane. This ratio can be determined in principle from the area of the narrow water peak relative to the total area under the proton spectrum, since the peak areas are proportional to the numbers of protons in the various components of the system. In practice, the broad component is difficult to measure reliably. Another measure for the water-proton content is the relative magnetization level in the water after complete spin diffusion, $I_{water}(t_m \rightarrow \infty)/I_{water}(t_m = 0)$. This ratio gives the fraction of the mobile water protons in the system, which was 0.32 (±0.04) in our system. The resulting effective water layer thickness in the simulation was 3 nm. The fast translational diffusion of the water molecules, which homogenizes the magnetization distribution in the water layer, was taken into account by a diffusion coefficient of 3 nm^2/ms. Choosing a larger diffusivity does not alter the observed diffusion into the membrane on the time scale of milliseconds, since the magnetization distribution in the water phase is already equilibrated within hundreds of microseconds.

The ^{1}H spectrum of Figure 3a shows that, in addition to the water signal at 4.9 ppm, there is a second narrow peak at 3.5 ppm, with an intensity of ca. 10% of the water peak. Its chemical shift is consistent with that expected for the methyl groups in the head-group choline in the lipid vesicles. The estimated ratio of mobile water to choline methyl protons is $\{2 \times 0.32\}:\{[9/(46 + 5 + 4 + 9)] \times 0.68 \times 3/5\} = 92:8$. The

(27) Schmidt-Rohr, K.; Spiess, H. W. *Multidimensional solid-state NMR and polymers*; Academic Press: London/San Diego, CA, 1994; pp 402−439.

(28) Buldt, G.; Gally, H. U.; Seelig, J.; Zaccai, G. *Nature* **1979**, *271*, 182−184.

(29) Wiener, M. C.; White, S. H. *Biophys. J.* **1992**, *61*, 434−447.

(30) Edzes, H. T.; Samulski, E. T. *J. Magn. Reson.* **1978**, *31*, 207−229.

Table 1. Simulation Parameters for the Spin-Diffusion Curves of Figures 1 and 5

One-Dimensional Spin Diffusion Parameters

layer	thickness (nm)	diffusion coefficient (nm^2/ms) 0.2-nm step size	0.1-nm step size
source region (H_2O)	3	≥3	
interface	0 (one step)	0.05	0.025
total lipid+protein	6	0.4	

Spin-Diffusion Curves

lipid detection regions	depth from solid−water interface (nm): protein-free bilayer surface	bilayer + protein surface
phosphate head groups	0.1 (60%)	1.6 (40%)
lipid acyl chains	0.6−1.9	2.1−3.6
lipid CH_3 groups	2.1 (70%)	3.8 (30%)

protein detection regions	depth from solid−water interface (nm)
amide backbone	0.5−1
lysine	−0.2 to +0.1 (20%)
	1.5−2 (80%)
amide side chains	0.5 (30%)
	2.5 (70%)

temperature-dependent line width and spin-diffusion behavior of the two peaks is similar, so that they can be treated together as a homogeneous source of mobile-species magnetization.

Magnetization Transfer across the Water−Solid Interface. A rate-limiting process in the observed spin diffusion is the transfer of ^{1}H magnetization from the water to the membrane because the mobility of the water weakens the dipolar couplings to the membrane. The rate parameter was determined by fitting the data of spin diffusion into the membrane as a whole and to specific regions of the lipid, such as the phosphate group or the acyl chains, whose location in the membrane is known. The slow transfer was represented by a diffusivity of $D = 0.05$ nm^2/ms in a layer of 0.2-nm thickness at the water−membrane interface. This diffusivity corresponds to an estimated transfer rate or coupling strength of $\Omega \approx 1$ kHz $= 1$/ms, according to $D = \Omega a^2$, with the transfer distance of $a = 0.2$ nm. This rate is in reasonable agreement with values estimated from water T_1 relaxation in similar systems.[30,31] Once the transfer rate has been determined from simulations of the spin diffusion to specific regions in the lipid, the only fit parameter for the spin diffusion to specific sites in the protein is their depth of insertion into the membrane.

Table 1 summarizes the parameters used in the spin-diffusion simulations. Virtually identical simulations are obtained for the two step sizes of 0.2 and 0.1 nm with the parameters given in the two upper columns in Table 1, which differ in the "diffusion coefficient" at the water−solid interface. While the diffusion coefficient for thick domains does not depend on the step size, both the diffusion coefficient D and the transfer rate $\Omega = D/a^2$ at the interface depend on the step size a ($D \sim a$, $\Omega \sim 1/a$): The interface of one 0.2-nm step would map into two 0.1-nm steps of a 4-fold transfer rate. However, we require the interface to consist of one step also at 0.1-nm step size. The single 0.1-nm step replacing the two 0.1-nm steps "in series" must have half the (4-fold) transfer rate, since the effective rate across two steps in series is one-half of the individual rates. The interfacial diffusion coefficient $D = \Omega a^2$ with 0.1-nm steps is thus half the value that it has with 0.2-nm steps.

The description of the surface as being totally flat is only an approximation. In reality, the surface of a protein or a lipid layer has a corrugation, with an estimated amplitude of 3 Å. In addition, some water molecules can penetrate past the lipid phosphate groups to the glycerol backbone.[28,29] However, for the magnetization-transfer process, the relevant thickness of the interface is the local "gap" of approximately 0.2 nm. This is consistent with the models considered in refs 30 and 31.

As indicated in the schematic of Figure 1, a corrugation of a larger amplitude must occur between the water-exposed protein surface and protein-free lipid head group regions. This does not affect depth measurements of sites very near the protein surface, since the local diffusion behavior is unaffected by the larger-scale heterogeneities. However, for sites at intermediate depth near a surface step, the diffusion behavior will be affected, which will lead to some deviation from the curves of Figure 1b. For these sites, the distance from the water−solid interface is not equal to the depth from the average bilayer surface. In other words, the direction of the closest distance to the water may not be along the bilayer normal. For these sites, the description of the system as a layered structure is not a particularly good approximation and the depth determination will be less reliable. On the other hand, for more deeply buried sites, the detailed surface features will be of limited effect.

A shortcoming of previous theoretical treatments of water−solid cross-relaxation[30] is that they neglected the thickness dependence of the "rate" of equilibration by spin diffusion. The correct time constant for a layer ~3-nm thick from surface to center can be estimated from $t = \langle x^2 \rangle / 2D \sim 10$ ms $= (100\ \text{Hz})^{-1}$, which is in good agreement with the time constant of the experimental water−solid magnetization exchange (Figure 3c). This rate is an order of magnitude slower than the spin-diffusion rate calculated by Edzes and Samulski,[30] who just considered the exchange rate between two neighboring protons. This difference is important in our system and probably also in the rehydrated steer-skin collagen that they investigated. In both systems, the spin-diffusion rate of ~100 Hz is probably the rate-limiting step for the water−solid magnetization exchange.

Possible mechanisms for the observed efficient magnetization exchange between water and solid include proton exchange[31] and dipolar magnetization transfer or cross relaxation[30] from bound water that exchanges with the mobile water. These processes can be distinguished by the temperature dependence of the transfer rate and the ^{1}H line width. While dipolar couplings become less efficient at higher temperatures due to the decreased residence time of the bound water, proton exchange rates would increase with temperature. At 240 K, the water line exhibits a homogeneous broadening of 300 Hz. We found experimentally that this line width decreases with increasing temperature and that the water−solid transfer rate decreases proportionally. This strongly suggests that the line broadening and magnetization exchange are dominated by dipolar couplings.

Effect of T_1 Relaxation. At long mixing times, the proton z-magnetization is decreased by T_1 relaxation. Its effect was determined by running the pulse sequence of Figure 2a with $\tau_d = 0$, i.e., without the mobility filter, and determining the decay of the magnetization as a function of t_m. In our sample, at $t_m = 50$ ms, the ^{1}H T_1 decay factors are 0.95, 0.85, and 0.72 for protons of the lipid acyl chains, protein backbone, and water layer, respectively. Thus, T_1 relaxation is not yet very significant at $t_m = 50$ ms, where the spin diffusion is nearly complete. For $t_m < 50$ ms, only minor T_1 corrections, achieved by division by the T_1 decay factors, are necessary. For longer mixing times,

(31) Hills, B. P. *Mol. Phys.* **1992**, *76*, 489−508.

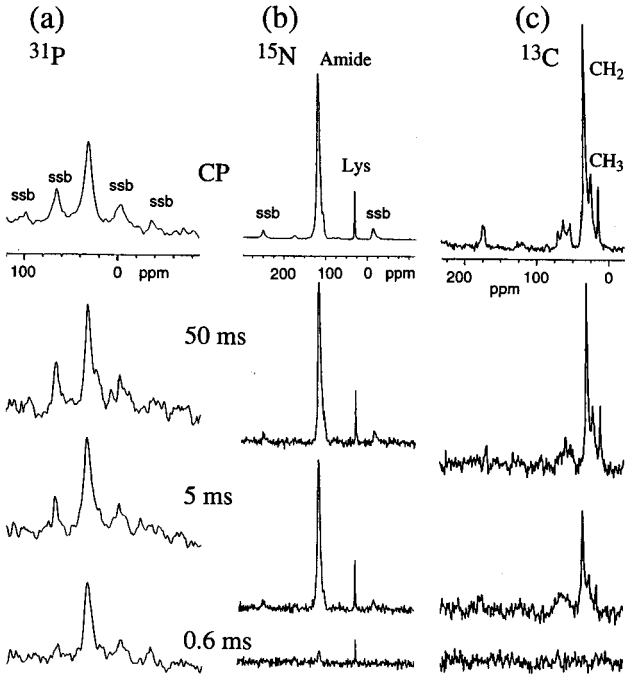

Figure 4. Cross-polarization and spin-diffusion magic-angle spinning spectra of the colicin−lipid−water system. Bottom to top: Spectra after 0.6, 5, and 50 ms of ^{1}H spin diffusion (1−2 h signal acquisitions). Top row: Cross-polarization spectra without spin diffusion, for reference. (a) ^{31}P spectra of lipid head groups, with spinning sidebands (labeled "ssb"). (b) ^{15}N spectra of the protein, displaying peaks of the backbone and side-group amides and the lysine side groups. (c) ^{13}C spectra of the lipid and protein, dominated by the signal of the lipid acyl chains at 34 ppm. The sharp signal of the CH_3 is observed at 15 ppm.

the magnetization is nearly equilibrated by spin diffusion and the further decay of the magnetization in the two experiments, with long and vanishing τ_d, will be proportional, regardless of how T_1 relaxation and spin diffusion combine. Thus, the decay factors of the reference experiment can be used as correction factors. For the same reasons, for $t_m > 200$ ms, spin diffusion makes the measured T_1 decay factors of all components nearly equal. Rather than correcting for it approximately, T_1 relaxation could also be included explicitly in the simulations. The two or three intrinsic T_1 relaxation times, of the mobile and solid phases, which are additional parameters in the simulations, can be determined by independent measurements, namely the relaxation curves of the magnetization in both phases without selection.

The main information content of the spin-diffusion data is not affected by the T_1 relaxation: Nearly the same T_1 correction is applied and applicable to both the reference lipid data and the protein data. As a consequence, the difference in their mixing-time dependence is unaffected by the T_1 correction.

Results

Figures 3−5 show representative spectra and corresponding magnetization-buildup curves for ^{1}H spin diffusion, starting from the mobile-water protons, as detected in different parts of the water−membrane system. The Goldman−Shen selection delay (^{1}H T_2 filter) was $\tau_d = 200$ μs. The traces for the ^{13}C-detected lipid acyl chains and the ^{31}P-detected phosphate head groups are clearly different. The magnetization from the mobile water reaches the phosphate groups first because they are closer to the membrane−water interface than the acyl chains. The curves through the data points in Figure 5 are spin-diffusion fits, with parameters as discussed above and summarized in Table 1. The

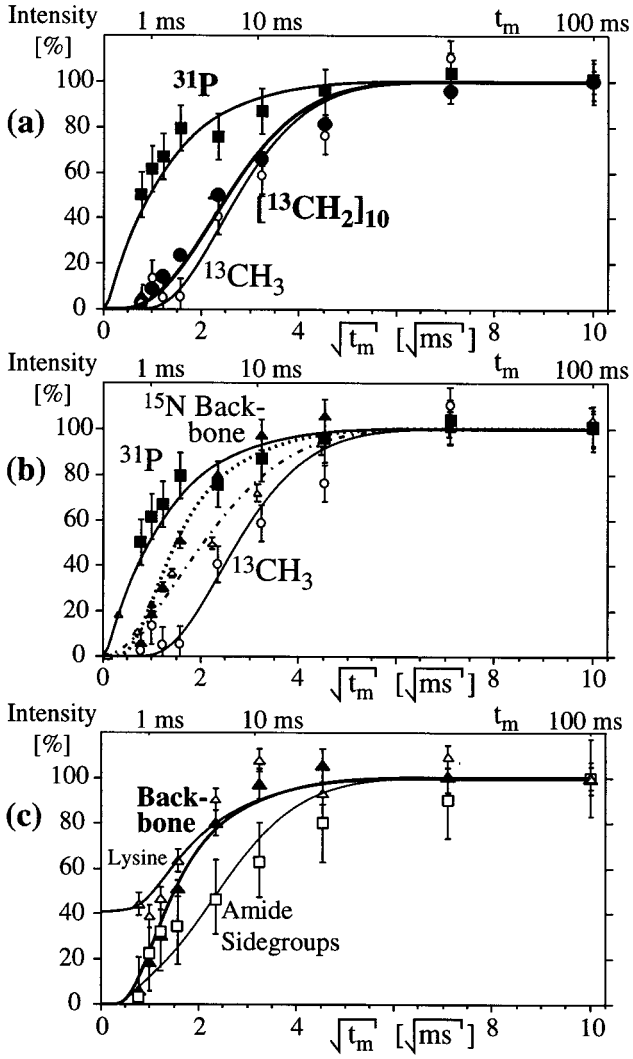

Figure 5. Time dependence of X-nucleus-detected ^{1}H spin-diffusion signal intensities in the colicin−lipid−water system, after selection by $\tau_d = 200$ μs in the Goldman−Shen sequence of Figure 2a. The data were derived from spectra including those shown in Figure 4. The minimum spin-diffusion time of 0.5 ms is half the cross-polarization contact time, during which the dipolar couplings are scaled in magnitude by 0.5. (a) Lipid data: phosphate head groups (■) from ^{31}P detection, lipid acyl chains (●), and CH_3-ω (○) from ^{13}C detection. (b) Comparison of lipid and protein spin diffusion: phosphate head groups (■) and lipid CH_3-ω (○), protein amide backbone (▲, dotted line) from ^{15}N detection**.** The overall magnetization in the solid, obtained as the complement of the water ^{1}H magnetization (Figure 3c) is shown as a dash−dotted line (△). (c) Data for different parts of the protein, as resolved in the ^{15}N spectrum (Figure 4b): amide backbone (▲), amide side chains (□), and lysine side chains (△). Aromatic and arginine signals were too small to be detected reliably. Intensities are measured as peak heights of the centerband. Integrated intensities of the center and sidebands are used for the ^{31}P data. All error bars are estimated as 75% of the peak-to-peak noise in the spectrum.

same parameters fit the decrease of the water magnetization observed in the proton spectrum (Figure 3c). Due to the conservation of overall z-magnetization, disregarding T_1 relaxation, the decrease of the water magnetization is exactly complementary to the overall increase of the immobile protons in the membrane. This increase of the ^{1}H magnetization in the lipid and protein is included in the plot of Figure 5b [open triangles, dash−dotted line].

Spin Diffusion into the Lipids. The t_m dependence of the ^{31}P and ^{13}C lipid signals (Figure 4a,c and Figure 5a) provides

references for comparison with the protein data, since the depths of these groups in the bilayer are known.[28] First, the lipid data are used to determine the water−solid transfer rate needed for the spin-diffusion simulations. The resolved ^{13}C signal of the lipid acyl chains includes eight CH_2 units, but excludes COO, CH_2-2, CH_3-ω, and CH_2-(ω-1) signals. Consequently, it provides a marker for the range 0.9−1.9 nm from the protein-free bilayer surface. The phosphate group is expected 0.4 nm from the protein-free bilayer surface.[28] However, due to the negative partial charge on the phosphate, water molecules may actually cluster at the phosphate group. The strong intensity of the phosphate resonance in the ^{31}P data at short spin-diffusion times t_m indicates that this is the case. Data for lipids in similarly prepared vesicles without adsorbed protein show similar time dependencies.

The ^{31}P data show an indication of a bimodal behavior. A very fast initial rise up to 75%, associated mostly with the centerband in the spectrum, is observed, followed by a slower rise at $t_m > 2$ ms, up to 100%, associated with an increase in sideband intensities. This effect is not unexpected in our sample. Colicin E1 is known to bind strongly to the lipid bilayer.[23] As a result, a considerable fraction of lipid head groups are blocked by the protein and thus inaccessible to the H_2O. Their magnetization rises only after the ^1H magnetization has traversed the protein or diffused within the bilayer from the water-accessible regions. It is likely that their motions are reduced, which would lead to less motional narrowing and more intense spinning sidebands. In the spin-diffusion fit, a ratio of the water-accessible to protein-covered lipids was set to 60:40 (±20). A ratio of at least 50:50 is expected, since 50% of the head groups are on the inside of the vesicles and therefore cannot be covered by the protein.

Spin Diffusion into the Protein and Dipolar Dephasing. Figures 4b,c and 5b show that the overall spin diffusion into the protein, as detected in the backbone amide ^{15}N groups, is significantly faster than into the lipid acyl chains or the overall protein−lipid system. This proves directly that most of the protein is on the surface of the membrane, consistent with both the "umbrella" and "penknife" structural models of the membrane-bound closed-channel state discussed in the Introduction. On the basis of the spin-diffusion data, the maximum fraction of protein deeply inserted into the lipid bilayer is 30%. This means that it is not possible from these data to distinguish between the two proposed models of membrane insertion of helices 8 and 9, which make up about 20% of all residues. Nevertheless, with specific isotopic labels (e.g., ^{13}C or ^{19}F) in these helices, the spin-diffusion technique promises to yield such information.

The spin-diffusion and $^1H-^{15}N$ dipolar-dephasing results for the protein backbone indicate depths and mobilities consistent with surface-associated α helices. Binding studies[23,32] have demonstrated that each colicin E1 channel domain binds to approximately 50 lipid molecules, which have a combined MW of 40 kDa in our system. Given this weight ratio, and the associated volume ratio assuming nearly equal densities, the protein thickness should be approximately half the single-lipid-layer thickness. Thus, the colicin E1 channel domain should have a thickness of approximately 1.2 nm, roughly consistent with the full diameter of an α helix. The spin-diffusion fit (Figure 5b and Table 1) yields a depth range of 0.5−1 nm for the amide backbone. This range corresponds to a 0.5-nm thickness, which is consistent with the diameter of an α-helical backbone. The minimum 0.5-nm depth is expected due to the side chains surrounding the backbone.

(32) Heymann, J. B.; Zakharov, S. D.; Cramer, W. A. *Biochemistry* **1996**, *35*, 2717−2725.

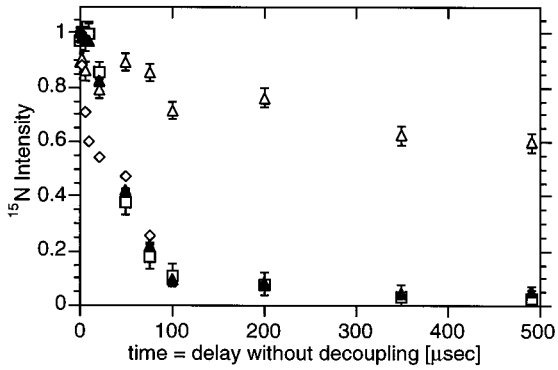

Figure 6. Time dependence of $^1H-^{15}N$ dipolar-dephasing signal intensities. Data were measured from spectra obtained with the pulse sequence of Figure 2b: overall backbone amide (▲); side chain amide (Gln and Asn) (□); lysine side chain (△); aromatic side chains (Trp and His) (◇). Aromatic data were collected with 1-ms contact times (for increased signal); all others were collected with 3-ms contact times. For clarity, the large error bars (±0.2) for the aromatic intensities are omitted.

Finally, the dipolar-dephasing experiment (Figure 6) shows that a small but nonvanishing fraction, 2−10%, of the protein backbone possesses significant mobility.[33] This fraction is likely to correspond to loosely bound, nonhelical portions of the structure. The overall low backbone mobility suggests that most of the protein backbone is structured or tightly bound to the membrane, consistent with trypsin proteolysis studies in which cleavage was not observed in the C-terminal 140 residues of P190.[34]

The depths and mobilities measured for side chains can in principle be used to identify the membrane and aqueous faces of surface-associated helices. In the colicin system, the 24 Lys side chains are divided between a mobile, surface-exposed fraction and an immobile, buried fraction. The signal of the Lys side chain displays a significant nonzero initial value in the spin-diffusion experiment (see Figure 5c). The T_2 of the lysine is longer than that of the rest of the protein but is shorter than that of water. Therefore, the nonzero initial intensity is likely to be due to incomplete suppression by the mobility filter. To augment this information, the $^1H-^{15}N$ dipolar-dephasing experiment provides a more quantitative estimate of the fraction of high-mobility lysine side groups, as shown in Figure 6. Even after long dephasing times of nearly 500 μs, the lysine signal remains at a level of ∼60%. This fraction must be located in a highly mobile environment, where the N−H dipolar couplings are efficiently averaged out by fast, nearly isotropic motions. It should be noted that the nitrogen-containing ends of the Lys side chains can have different mobility than the backbone, since they are separated by a flexible $(CH_2)_4$ "spacer". The rate of the initial decay in the dephasing curve of the lysines is similar to that of the backbone, indicating that ∼40% of the lysines are relatively immobile. In the spin-diffusion data, the increase of the lysine signal with t_m indicates that this rigid portion of the lysines are buried.

The spin-diffusion and dipolar-dephasing experiments provide important complementary information for highly mobile segments, such as a large fraction of the Lys residues. In the spin-diffusion experiment, high mobility leads to both incomplete suppression in the T_2 filter and inefficient cross-polarization.

(33) The single proline (which has weak dipolar coupling due to no attached proton rather than to mobility) would make an insignificant contribution to the 2−10% fraction, justifying the interpretation that this fraction is mobile.

(34) Zhang, Y.-L.; Cramer, W. A. *Protein Sci.* **1992**, *1*, 1666−1676.

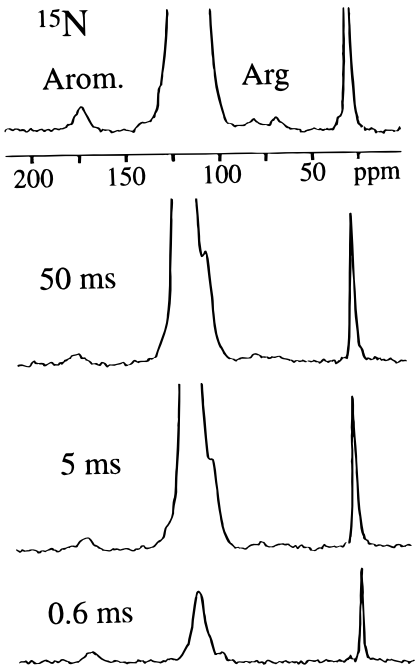

Figure 7. ^{15}N spectra after 70-μs T_2 filter in the Goldman−Shen experiment, after 0.6, 5, and 50 ms of ^{1}H spin diffusion. The cross polarization spectrum is shown at the top for reference. The peak of the ^{15}N in aromatic side groups, to the left of the dominant amide signal, is observed already at very short mixing times. The two small peaks corresponding to the arginine appear to increase in a manner similar to that of the backbone amide signal.

These two effects compromise any quantitative study of the mobile groups by weighting the build-up curve toward the less mobile groups. Thus we have used the dipolar-dephasing experiment to estimate the mobile fraction (60%), while the spin-diffusion experiment demonstrates that a significant fraction of the less mobile lysine side groups are buried away from the interface.

The ^{15}N signal of the amide side chains of glutamine (Gln) and asparagine (Asn) residues is observed in Figure 4b as a peak near 105 ppm that partly overlaps with the dominant amide-backbone band. Figure 5c shows that, after a fast initial rise to about 30% of the final value, this signal increases more slowly than that of the backbone amides. This indicates that 50−70% of these side groups are buried below the average depth of the amide backbone, consistent with the results of the spin-diffusion simulation. This finding is consistent with the small mobility of these residues demonstrated by the dipolar-dephasing experiment, where the behaviors of the side chain and backbone amide intensities are very similar.

The aromatic (His and Trp) and arginine side-group signals are too weak to be observed in the spectra of Figure 4. However, they are detected above the noise in experiments with a weaker ^{1}H T_2 filter of $\tau_d = 70$ μs, which suppresses less of the water magnetization (Figure 7). The His and Trp residues show significant intensity at the shortest mixing times, indicating that a significant fraction is located close to the membrane−water interface. In contrast to the lysines, the His and Trp residues display a dipolar-dephasing behavior that does not indicate high mobility, which is not surprising for these bulky side chains. The arginine signal in Figure 7 seems to rise together with the amide signals, indicating that this residue is not exposed to the surface. However, the low signal-to-noise of this peak does not allow quantification.

Discussion

Our experiments demonstrate that the spin-diffusion method described herein has promise as a versatile new tool for elucidating the structure of membrane-bound proteins. All of the spin-diffusion data, whether for the phosphate head groups, the lipid carbons, or the uniformly-^{15}N-labeled protein, are measured using the same sample. The samples are prepared for study by inserting the protein into unilamellar lipid vesicles, for which protocols are well-defined.

The simulations demonstrate that spin diffusion with a single set of reasonable parameters can be used to describe the experimental data. For the fits to the lipid data, only one variable, the water−solid transfer rate, is relatively free. All other domain-thickness and diffusion-coefficient parameters are constrained to a narrow range of allowed values, based on known properties of the system. The fit to the protein backbone data gives an average depth, due to the large number of overlapping sites. The depth of 0.5−1 nm that produces the curve shown in Figure 5b,c means that most of these sites are near, but not directly at, the surface. The depths given have an estimated uncertainty of ±0.3 nm.

In uniformly labeled proteins, like the ^{15}N-enriched colicin E1 channel-forming domain (P190) used in this study, the spin-diffusion technique contributes to the determination of the membrane location of the protein, whether surface-associated, integral, or with significant components of both. For a surface-bound protein, the time dependence of the spin diffusion will be similar to that of the phosphate head groups in the lipids, detected conveniently by ^{31}P NMR. Proteins that insert deeply into the lipid bilayer will show longer induction times and reach their equilibrium states later than the surface sites do. Such "buried" structures can be identified directly by comparing with spin-diffusion data obtained for the hydrophobic lipid chains, with detection of ^{13}C in natural abundance.

It should be emphasized that, as demonstrated above, the depth of insertion can be obtained for any site with spectrally resolved peaks. For example, analysis of the population of the side chain amines of the lysines yields information as to the proximities of these groups to the interface. It has also been demonstrated that depth profiling is feasible for resolved sites that occur less frequently, like the side-chain amides, the ^{15}N-containing aromatic side chains, or even the single arginine. The signal-to-noise ratio, which is low for these rarely occurring residues, can be improved by performing the experiments with smaller sample rotors for a better filling factor, by an increased amount of sample in the 7-mm rotors, or by enrichment and detection of ^{13}C, which is a more sensitive nucleus than ^{15}N. Sensitivity would also be greatly enhanced with the incorporation of ^{19}F-labeled amino acids.

For future studies of the colicin E1 channel-forming domain and other membrane-bound proteins, additional information can be obtained by utilizing isotopic labels at a specific site in a unique amino acid. In particular, isotopic labeling of an amino acid that occurs only once in the wild type or in a mutant is conceivable. The spin-diffusion measurements would then determine the depth of insertion of this site into the lipid bilayer. For example, a number of single Cys and single Trp mutant proteins of the colicin E1 channel-forming domain have been constructed.[35−37] The spin-diffusion curves for these targeted

(35) Lakey, J. H.; Baty, D.; Pattus, F. *J. Mol. Biol.* **1991**, *218*, 639−653.
(36) Steer, B. A.; Merrill, A. R. *Biochemistry* **1994**, *33*, 1108−1115.
(37) Shin, Y.-K.; Levinthal, C.; Levinthal, F.; Hubbell, W. L. *Science* **1993**, *259*, 960−963.

sites would test various structural models for the bound state as described above.[16] Again, as with the uniformly labeled material, auxiliary data on the water protons, the lipid carbons, and the head-group phosphates would calibrate the depth measurements in a single sample. Generally, two kinds of depth resolution need to be distinguished: The relative depth of two residues in the same sample can be determined with relatively high accuracy. The simulation in Figure 1b shows that, at depths smaller than 1.2 nm, the expected difference in the diffusion curves is sufficiently large that a depth difference of 0.2 nm should be resolved if the signal-to-noise ratio is similar to that of the experimental data shown here. The resolution is lower in the center of the membrane, where a region of approximately ±0.5 nm shows the same mixing-time dependence. This reduced spatial resolution is due to the vanishing spatial variation of the magnetization, $dM/dz = 0$, at the center, imposed by the symmetry of the magnetization transfer from both sides of the membrane. Measurements of absolute depth and comparisons between different samples are expected to have a larger error due to variations of sample parameters such as water content and water−solids transfer rate.

The spin-diffusion experiment may be further optimized at lower temperatures. The crucial step in the transfer of magnetization from the water to the protein−lipid layer occurs at their interface. If this transfer is slower than equilibration by spin diffusion within the solid layer, all sites in the protein and lipid show the same spin-diffusion time dependence and no depth resolution can be achieved. Simulations confirm that the depth resolution increases strongly with the water−solid transfer efficiency. For optimizing the depth resolution of the experiment, it will be useful to make the transfer process even more efficient by decreasing the temperature below 240 K, the minimum sample temperature with the low-temperature apparatus used in our experiments.

The ^{1}H spin-diffusion experiment described here can be used in conjunction with various other NMR methodologies after cross polarization. For instance, these techniques can be aimed at discriminating between sites that have overlapping signals in the X-nucleus 1D spectrum, by two-dimensional correlation which identifies a specific sequence of residues in the surface-associated, solvent-accessible region of the protein. Spin diffusion can also be applied to select a particular region in the protein−lipid system, e.g. the surface-associated population, and characterize its structural or dynamic parameters. For example, the spin-diffusion approach could be combined with double-quantum techniques[8] to measure the torsion angles of sites close to the water layer.

Summary and Outlook

We have shown that mobile water at 240 K is a suitable source of magnetization for ^{1}H spin-diffusion experiments in gel-phase lipid vesicles with bound protein. The transfer from water to proteins and lipids is fast enough to allow for significant depth resolution in the membrane, demonstrated experimentally by ^{1}H, ^{13}C, ^{15}N, and ^{31}P detection of the proton magnetization at various depths in the protein and lipid layers. In the colicin E1 channel-forming domain investigated here, most (>70%) of the protein is located at the surface of the lipid bilayer. The data show that ca. 60% of the 24 lysine side groups in the system are highly mobile and probably solvated at the surface of the protein. We have presented spin-diffusion simulations that reproduce the lipid reference data well, with only one free parameter, and are useful for estimating the depth of insertion of protein residues. With specific isotopic labels in a potential transmembrane region of a protein, it will be possible to determine the depth of insertion of individual residues in the membrane.

Acknowledgment. Partial financial support by the National Science Foundation, Materials Research Science and Engineering Center, is gratefully acknowledged. This research was supported by U.S. Public Health Service Grant GM47601, an award from Research Corporation, and an NSF Young Investigator Award to L.K.T. K.S.-R. thanks the Arnold and Mabel Beckman Foundation for a generous Young Investigator Award. W.A.C. was supported by NIH GM-18457. The NMR instrument was purchased with a grant from the NSF (BIR-911996) and funds from the University of Massachusetts and is partially supported by the NSF Materials Research Science and Engineering Center Facility at the University. We thank Dr. L. Charles Dickinson for technical support of the NMR Facility and Dr. S. Schendel and T. Wu for preparation of labeled P190.

JA972655E